Microchimica Acta
https://doi.org/10.1007/s00604-018-2808-4

ORIGINAL PAPER

Photoelectrochemical biosensor for microRNA detection based on multiple amplification strategies

Minghui Wang[1] · Huanshun Yin[1] · Yunlei Zhou[1] · Jingrui Han[1] · Tingqun He[1] · Lin Cui[2] · Shiyun Ai[1]

Received: 24 January 2018 / Accepted: 14 April 2018

Abstract

A photoelectrochemical biosensor is described for sensitive detection of microRNA-162a. A multiple amplification strategy is employed that involves (a) isothermal strand displacement polymerase reaction; (b) terminal deoxynucleotidyl transferase-mediated extension, (c) amplification of streptavidin-coated gold nanoparticles, and (d) biotin functionalized alkaline phosphatase. Graphite-like C_3N_4 (g-C_3N_4) nanosheets were used as photoactive material. By using these amplification strategies, the detection limit is as low as 0.18 fM of microRNA, and the photocurrent increases linearly with the concentration of microRNA-162a in the range from 0.5 fM to 1 pM. The method was successfully applied to quantify the expression level of microRNA-162a in total RNA extracted from the leaves of maize seedlings after incubation with the chemical mutagen ethyl methanesulfonate. The results confirmed the applicability of the method to the analysis of practical biological samples.

Keywords Isothermal strand-displacement polymerase reaction · Terminal deoxynucleotidyl transferase-mediated extension · Streptavidin coated gold nanoparticles · Biotin functionalized alkaline phosphatase · Chemical mutagen

Introduction

MicroRNAs are short, single-stranded, non-coding RNAs with a length of about 22 nucleotides. They play important roles in gene expression, cell development, cell differentiation and cell apoptosis [1, 2]. Due to their short length, high sequence homology, low cellular abundance and easy degradability, it is a challenge to realize the sensitive detection of microRNAs [3]. Therefore, an effective method to achieve sensitive detection of microRNAs is necessary. Various analytical methods have been developed, such as Northern blotting [4, 5], microarrays [6, 7], electrochemistry [8, 9] and fluorometry [10–12]. Although most of them are sensitive, it is still challenging for microRNA detection due to the unique properties of microRNA, including short lengths, low abundance and susceptibility to degradation. Therefore, it is urgent to develop a rapid, convenient, reliable and ultrasensitive analytical method for microRNAs detection.

Photoelectrochemical (PEC) sensors have attracted attention due to their excellent sensitivity and low background [13]. As an important part of PEC biosensors, photosensitive materials are critical to sensor performance. So far, the commonly applied photoactive materials are metal-containing semiconductors, such as Bi_2S_3, CdS, TiO_2, ZnO, etc. [14, 15]. These materials exhibited good detection performance but may lead to environmental pollution due to the metal components they contain. Therefore, it is of great significance to find a new environmentally friendly photosensitive material. With a two-dimensional layered structure like graphene, g-C_3N_4 nanosheets has been successfully applied in photocatalysis or PEC biosensing because of the large surface area and rapid charge transfer. In addition, g-C_3N_4 has the advantages of nontoxicity, excellent chemical stability, visible

Electronic supplementary material The online version of this article (https://doi.org/10.1007/s00604-018-2808-4) contains supplementary material, which is available to authorized users.

✉ Huanshun Yin
yinhs@sdau.edu.cn

✉ Yunlei Zhou
zhyl@sdau.edu.cn

[1] College of Chemistry and Material Science, Shandong Agricultural University, Taian 271018, People's Republic of China

[2] College of Chemistry, Chemical Engineering and Materials Science, Collaborative Innovation Center of Functionalized Probes for Chemical Imaging in Universities of Shandong, Key Laboratory of Molecular and Nano Probes, Ministry of Education, Shandong Provincial Key Laboratory of Clean Production of Fine Chemicals, Shandong Normal University, Jinan 250014, People's Republic of China

Published online: 20 April 2018

light response and unique semiconductor properties [16]. In our previous work, we have developed a photoelectrochemical biosensor for microRNA detection based on g-C_3N_4 [17], which showed excellent detection performance, but still not sensitive enough. To further enhance the sensitivity of the biosensors, we can combine some signal amplification strategies.

Isothermal chain-displacement polymerase reaction (ISDPR) is a process that uses an isothermal amplification process to produce a large number of products to amplify the detection signal [18]. Terminal deoxynucleotidyl transferase (TdT) is a unique DNA polymerase that can catalyzes the sequential addition of dNTPs to the 3′-OH group of oligonucleotide primers to produce specific sequences such as poly-T ssDNA [19]. Both methods can effectively amplify the signal, so when ISDPR combined with the TdT-mediated extension, the sensitivity of the biosensor may be improved effectively.

Herein, we describe a multiple amplification method for microRNA detection, which integrated isothermal strand-displacement polymerase reaction (ISDPR), TdT-mediated extension and the amplification of streptavidin-coated gold nanoparticles (SA-AuNPs) and biotin-modified alkaline phosphatase (ALP). ISDPR and the TdT-mediated extension strategy were introduced to this work to amplify the signal by generating or extending DNA strands. In addition, the amplification of SA-AuNPs and biotin-ALP were also involved. This greatly improves the photocurrent response by catalyzing the hydrolysis of AAP to produce electron donor of AA. The method was used to investigate the effect of the chemical mutagen ethyl methanesulfonate (EMS) on the expression level of microRNA-162a in the leaves of maize seedlings. These results confirmed the applicability of the method in practical biological samples.

Experimental section

Materials and reagents

Phi29 DNA polymerase, Nt.BsmAI nicking endonuclease and terminal deoxynucleotidyl transferase (TdT) was received from New England Biolabs (Ipswich, MA, https://www.neb.com). Ascorbic acid-2-phosphate (AAP), hydrogen tetrachloroaurate trihydrate ($HAuCl_4 \cdot 3H_2O$), dithiothreitol (DTT), tris(hydroxymethyl)aminomethane (Tris), ethyl methanesulfonate (EMS) and tris (2-carboxyethyl) phosphine hydrochloride (TCEP) were purchased from Aladdin (Shanghai, China, http://www.aladdin-e.com). TRIzol® Plus RNA Purification Kit was obtained from Thermo Fisher (USA, https://www.thermofisher.com). PEG-3350 was received from Solarbio (China, http://www.solarbio.com). Biotin-ALP, biotin-dUTP, and the synthetic DNA were purchased from Sangon (Shanghai, China, https://www.sangon.com). HPLC-purified microRNAs were provided by Takara (Dalian, China, http://www.takara.com.cn). The nucleotide sequences are listed as follows. Template DNA, 5′-CAC ACT GCA CTT TTT AGC ACG GCG AGA CTG GAT GCA GAG GTT TAT CGA; probe DNA, 5′-CAC ACT GCA CTT TTT AGC ACG G-$(CH_2)_6$-SH-3′; microRNA-162a, 5′-UCG AUA AAC CUC UGC AUC CAG-3′; single-base mismatched microRNA, 5′-UCG AUA AUC CUC UGC AUC CAG-3′; three-base mismatched microRNA, 5′-UCG AUC AAC CAC UGC CUC CAG-3′; non-complementary DNA, 5′-ACT CTC GAT CCC AGA TCT AGC-3′; microRNA-166e, GGA AUG UUG UCU GGU UCA AGG; microRNA-172a, 5′-AGA AUC UUG AUG AUG CUG CA-3′; microRNA-156d, 5′-UGA CAG AAG AGA GUG AGC AC-3′; microRNA-169a, CAG CCA AGG AUG ACU UGC CGA. Synthetic DNA and microRNA were dissolved in TE buffer (pH 7.4) and stored at −20 °C according to the manufacturer's instructions. All reagents were analytically pure grade.

The buffers employed in this work are as follows. TE buffer, 10 mM Tris-HCl and 1 mM EDTA (pH 7.4). MicroRNA hybridization buffer: 1 × SSC (15 mM sodium citrate and 0.15 M sodium chloride). Phi29 DNA polymerase reaction buffer: 10 mM $(NH_4)_2SO_4$, 50 mM Tris-HCL, 10 mM $MgCl_2$, 4 mM DTT, 200 μg mL^{-1} BSA (pH 7.5). Nt.BsmAI reaction buffer: 20 mM Tris-acetate, 50 mM potassium acetate, 10 mM magnesium acetate, 100 μg mL^{-1} BSA (pH 7.9). TDT reaction buffer: 20 mM Tris-acetate, 50 mM potassium acetate, 10 mM magnesium acetate, 0.25 mM $CoCl_2$, 100 μg mL^{-1} BSA, pH 7.9. Probe immobilization buffer: 10 mM Tris-HCl, 1.0 M NaCl, 1.0 mM TCEP and 1.0 mM EDTA (pH 7.4). DNA hybridization buffer, 1.0 mM EDTA, 10 mM Tris-HCl and 1.0 M NaCl (pH 7.4). Washing buffer, 10 mM Tris–HCl containing 50 mM NaCl (pH 7.4). PEC detection buffer: 10 mM Tris–HCl containing 50 mM KCl, 10 mM AAP and 0.1 mM $Mg(NO_3)_2$ (pH 9.8). Electrochemical impedance spectrum (EIS) detection buffer: 10 mM Tris-HCl containing 5 mM $K_3[Fe(CN)_6]$, 5 mM $K_4[Fe(CN)_6]$ and 0.1 M KCl (pH 7.4). All of the solution and redistilled deionized water were prepared with DEPC and autoclaved to protect from RNase degradation.

Synthesis of g-C_3N_4 and streptavidin-coated gold nanoparticles

The synthesis of g-C_3N_4 was based on a typical experiment as described in [20], and SA-AuNPs was prepared according to our previous report [21] (detailed description is shown in Electronic Supporting Material).

Isothermal strand-displacement polymerase reaction

20 μL of microRNA-162a, 20 μL of 1 μM template DNA, and 10 μL of microRNA hybridization buffer were first mixed. The mixed solution was heated to 95 °C for 5 min, and then it was cooled naturally to room temperature. After that, the solution was incubated for 2 h to insure the complete hybridization of DNA and microRNA.

After the addition of 10 μL of 250 U·mL^{-1} phi29 DNA polymerase, 10 μL of 250 U·mL^{-1} Nt.BsmAI, 10 μL of 500 μM dNTPs and 20 μL 5 × reaction buffer (0.25 M Tris-HCL, 50 mM $MgCl_2$, 50 mM $(NH_4)_2SO_4$, 20 mM DTT, 1 mg·mL^{-1} BSA, 0.25 M KCl), the mixture was incubated for 2.5 h at 37 °C. Finally, the reaction system was terminated with incubation at 65 °C for 10 min. The products were noted as amplified DNA (a-DNA) and stored at 4 °C.

PEC biosensor fabrication

The ITO conductive glass was cut into 1 cm × 5 cm size slices, and then cleaned according to our previous report [22]. 2 mg of g-C_3N_4 powder was dispersed in 1 mL double distilled deionized water and ultrasonicated for 20 min. Then, 40 μL of the g-C_3N_4 suspension was dropped on the bare ITO electrode surface. After being dried under infrared lamp irradiation, the prepared g-C_3N_4/ITO was rinsed with double distilled deionized water for three times. Then, 20 μL of AuNPs were further dropped on g-C_3N_4/ITO electrode surface and dried under infrared lamp irradiation, followed by rinsed with double distilled deionized water for three times (The electrode was noted as AuNPs/g-C_3N_4/ITO).

Subsequently, 20 μL probe immobilization buffer containing 1 μM probe DNA was dropped on AuNPs/g-C_3N_4/ITO electrode surface and incubated overnight at room temperature under humid condition. The obtained electrode was noted as ssDNA/AuNPs/g-C_3N_4/ITO. After rinsed with washing buffer for three times, 20 μL DNA hybridization buffer which containing the products of ISDPR (a-DNA) was dropped on the surface of ssDNA/AuNPs/g-C_3N_4/ITO and incubated for 2 h at 37 °C. The electrode (It was named as dsDNA/AuNPs/g-C_3N_4/ITO) was rinsed with washing buffer for three times. Afterward, the electrode was incubated with 20 μL of enzymatic amplification solution including 100 U mL^{-1} TdT, 20 μM biotin-dUTP and 1 × TdT reaction buffer for 2 h at 37 °C, and the obtained electrode was named as biotin/dsDNA/AuNPs/g-C_3N_4/ITO. After rinsed with washing buffer, the electrode was incubated with 20 μL SA-AuNPs for 1 h at moist conditions, and the electrode was noted as SA/biotin/dsDNA/AuNPs/g-C_3N_4/ITO. Subsequently, 20 μL of 0.1% PEG-3350 was dropped on the electrode surface and incubate for 30 min. After that, the electrode was further incubated with 20 μL biotin-ALP solution for 2 h. Finally, the electrode was rinsed with washing buffer and noted as ALP/SA/biotin/dsDNA/AuNPs/g-C_3N_4/ITO.

PEC detection

PEC measurements were performed with a homemade PEC system. A 500 W Xe lamp photo source was used as the irradiation source (Beijing Ceaulight Technology Co., LTD., China). Photocurrent was recorded on a CHI832A electrochemical workstation (Austin, USA) with a three-electrode system. A modified ITO electrode with an area of 0.195 cm^2 was used as the working electrode, a platinum wire as the counter electrode and a saturated calomel electrode (SCE) as the reference electrode. After the detection buffer was incubated with ALP/SA/biotin/dsDNA/AuNPs/g-C_3N_4/ITO at 37 °C for 30 min, the PEC response was recorded at visible light with an applied potential of −0.3 V.

Electrochemical impedance spectroscopy (EIS) was measured with a CHI660C electrochemical workstation (Austin, USA) in 10 mM Tris-HCl containing 5 mM $K_3[Fe(CN)_6]$, 5 mM $K_4[Fe(CN)_6]$ and 0.1 M KCl (pH 7.4) with the frequency range of 10^{-1}-10^5 Hz.

Sample preparation

Mature seeds of maize were used in this work. These maize seeds were separated into two groups with one group as detection sample and the other as control sample. The detection sample was immersed in ethyl methanesulfonate (EMS) solution at a concentration of 0.7% for 6 h. The control sample was immersed in distilled deionized water for the same time. Then, these seeds were washed in running water for 4 h. Afterwards, the seeds were embedded in gauze within petri dishes and cultured with double-distilled ionized water for a few days for germination. Finally, the leaves of the seedlings were harvested for RNA extraction by using TRIzol® Plus RNA Purification Kit according to the manufacturer' instructions. The concentration of the extracted RNA was analyzed by UV–vis spectrophotometry. For microRNA detection, the extracted RNA was diluted to the same concentration.

Results and discussion

Detection strategy

In this work, a photoelectrochemical biosensor was developed for microRNA-162a detection based on multiple amplification strategies. The fabrication process is illustrated in Scheme 1. Firstly, target microRNA-162a hybridizes with

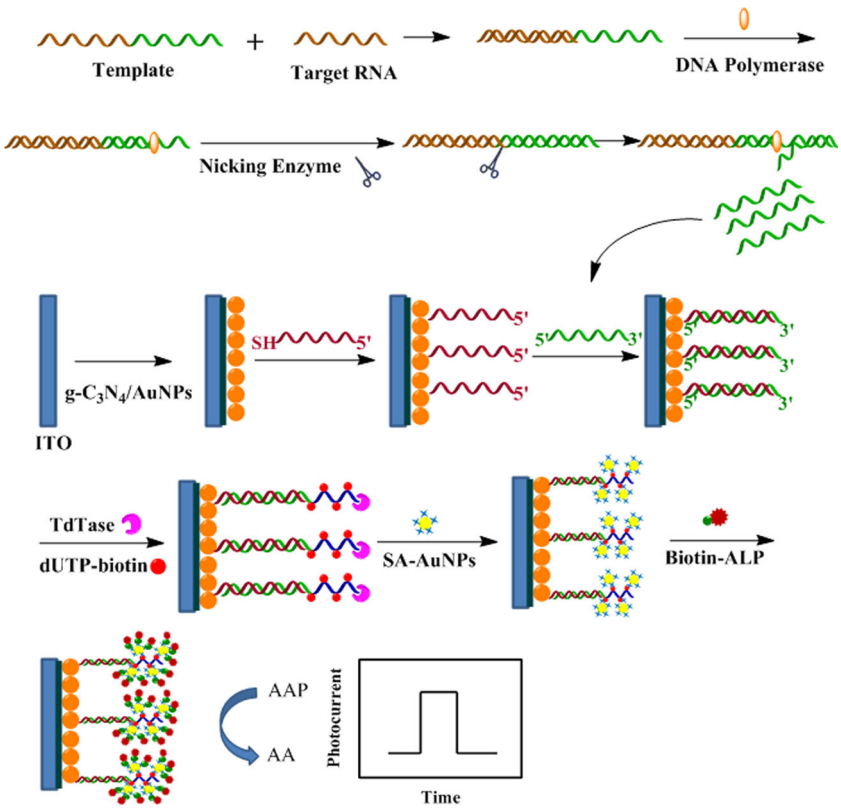

Scheme 1 Schematic illustration of the PEC biosensor fabrication process

template DNA and initiates isothermal strand-displacement polymerase reaction (ISDPR) from the 3′-end to form a double-stranded DNA in the presence of phi29 and dNTPs. Simultaneously, the recognition site for the Nt.BsmAI nicking endonuclease is generated, which induces Nt.BsmAI to incise a gap at the double-stranded DNA. Subsequently, the 3′ terminal of microRNA-162a is extended and the downstream DNA strand (named as a-DNA) would be replaced and released. As a result, a great number of a-DNA can be produced and may participate in the following reaction. Afterwards, g-C_3N_4 and AuNPs are immobilized on the bare ITO electrode surface through physical adsorption. Then, the thiol modified DNA (probe DNA) is self-assembled on AuNPs/g-C_3N_4/ITO surface by Au-S bond. Afterwards, a-DNA hybridizes with probe DNA on the electrode surface and trigger the TdT-mediated extension to fabricate long ssDNA of poly-U sequences containing lots of biotin. Depending on the high accuracy of TdT, dUTP-biotin is only added to the 3′-OH terminal of dsDNA, i.e. the terminal of a-DNA. Subsequently, the SA-AuNPs are attached to the electrode by the specific reaction between streptavidin and biotin. Finally, biotin-ALP is connected to the electrode surface and catalyzes the hydrolysis of AAP to produce AA, which lead to a strong photocurrent response.

The main advantage of this method is its high detection sensitivity due to the use of four kinds of signal amplification strategies, isothermal strand-displacement polymerase reaction, TdT-mediated extension, the amplification of SA-AuNPs and Biotin-ALP. ISDPR has the advantages of high efficiency and adaptability. TdT-mediated extension presents a facile, direct, and cost-effective way for miRNA detection. Furthermore, the amplification of SA-AuNPs and Biotin-ALP greatly improves photocurrent response. Based on these four kinds of signal amplification strategies, this PEC biosensor can achieve an ultrasensitive detection for target microRNA.

Characterization of materials

The morphologies of g-C_3N_4 and AuNPs were characterized by TEM. Figure 1a shows that the g-C_3N_4 contains a wrinkled-layer structure with several stacking layers, which was consistent with the literature report [23]. Figure 1b shows the morphology of the prepared AuNPs. Figure 1b shows the AuNPs to have an average diameter of approximately 20 nm.

Characterization of the biosensor

Electrochemical impedance spectroscopy (EIS) was used to monitor the fabrication process of the biosensor. Figure 2a shows that the bare ITO electrode has an interface electron transfer resistance (R_{et}) of about 80 Ω (curve a). The R_{et} value decreases obviously when g-C_3N_4 is modified on the ITO electrode surface (curve b), which may be ascribed to the

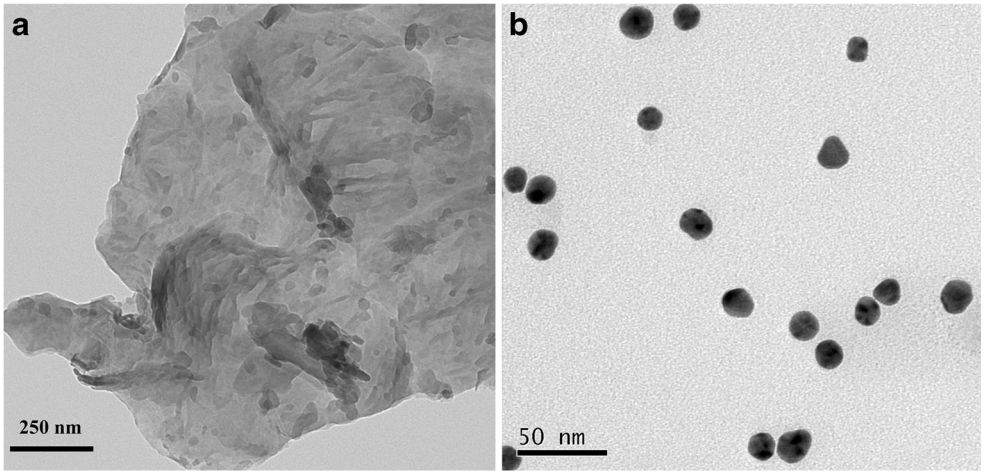

Fig. 1 TEM images of g-C_3N_4 (**a**) and AuNPs (**b**)

immobilization of g-C_3N_4, which increases the effective surface area of the electrode, and improves the diffusion efficiency of the redox probe to electrode. In addition, the amino group of g-C_3N_4 can also promote the diffusion of negative charged redox probe of $[Fe(CN)_6]^{3-/4-}$ to the electrode surface. After AuNPs is modified on the electrode surface, only a small semi-circle with a R_{et} of about 50 Ω is observed (curve c), indicating that AuNPs can increase the electrode conductivity and facilitate the electron transfer. Moreover, AuNPs can also improve the capture efficiency of probe DNA by increasing the surface area of the effective electrode. When probe DNA (curve d) and a-DNA (curve e) are sequentially attached to the electrode surface, a significant increase of R_{et} can be observed. These increases are due to the electrostatic repulsion between the negatively charged phosphoric acid backbone of oligonucleotides and the negatively charged $[Fe(CN)_6]^{3-/4-}$. Afterwards, the R_{et} value increases further when the electrode is incubated with TdT in the presence of dUTP-biotin (curve f), which may be attributed to the formation of long ssDNA, enhanceding the electrostatic repulsion between the oligonucleotides and the $[Fe(CN)_6]^{3-/4-}$. When SA-AuNPs is connected to the electrode, R_{et} increases distinctly (curve g). It is attributed to the fact that SA-AuNPs with a large size can hinder the diffusion of $[Fe(CN)_6]^{3-/4-}$ towards electrode surface. Similarly, when biotin-ALP is conjugated with SA-AuNPs on the electrode surface (curve h), R_{et} increases largely. It is ascribed to the steric hindrance of ALP, which limits the diffusion of $[Fe(CN)_6]^{3-/4-}$ to the electrode surface. These results indicate the successful fabrication of the biosensor.

Detection feasibility

The detection feasibility was monitored by the photocurrent response of different modified electrodes in 10 mM Tris-HCl containing 50 mM KCl, 10 mM AAP and 0.1 mM $Mg(NO_3)_2$ (pH 9.8). As illustrated in Fig. 2b, after g-C_3N_4 and AuNPs are

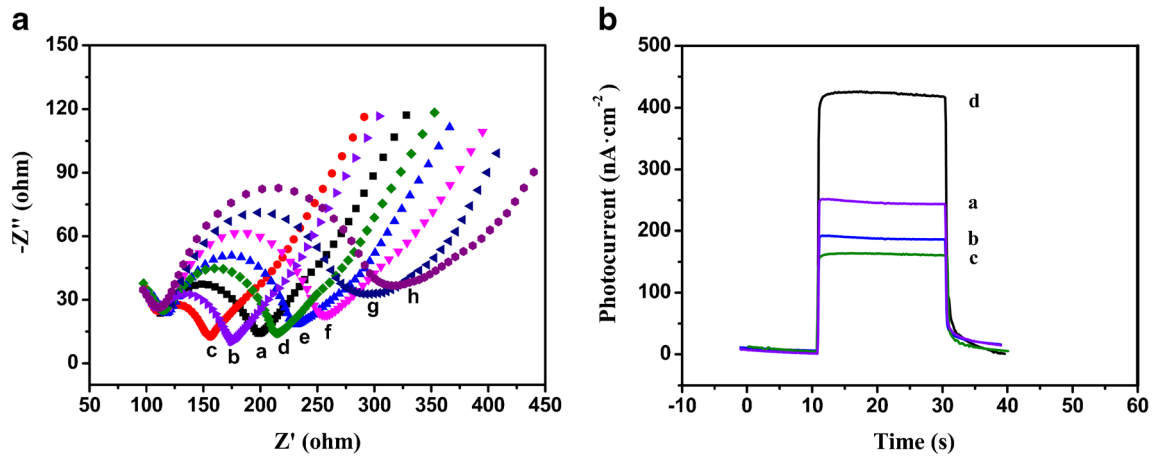

Fig. 2 **a** EIS of ITO (a), g-C_3N_4/ITO (b), AuNPs/g-C_3N_4/ITO (c), ssDNA/AuNPs/g-C_3N_4/ITO (d), dsDNA/AuNPs/g-C_3N_4/ITO (e), biotin/ssDNA/AuNPs/g-C_3N_4/ITO (f), SA/biotin/dsDNA/AuNPs/g-C_3N_4/ITO (g), ALP/SA/biotin/dsDNA/AuNPs/g-C_3N_4/ITO (h) in 5 mM $[Fe(CN)_6]^{3-/4-}$ (1:1) solution containing 0.1 M KCl. **b** The photocurrent response of AuNPs/g-C_3N_4/ITO (a), ssDNA/AuNPs/g-C_3N_4/ITO (b), SA/biotin/dsDNA/AuNPs/g-C_3N_4/ITO (c), ALP/SA/biotin/dsDNA/AuNPs/g-C_3N_4/ITO (d) in 10 mM Tris-HCl containing 50 mM KCl, 10 mM AAP and 0.1 mM $Mg(NO_3)_2$ (pH 9.8)

modified on the electrode (curve a), a weak photocurrent can be observed, which may be attributed to the absence of a valid electron donor. When probe DNA (curve b) is assembled to the electrode surface, the photocurrent decreased. It is due to the steric hindrance of oligonucleotides, which decreases the electron-transfer efficiency. Similarly, after SA-AuNPs connects to the electrode, the photocurrent further decreases (curve c). It is also due to the fact that the steric hindrance decreases the electron-transfer efficiency. Subsequently, the photocurrent response increases significantly after the immobilization of biotin-ALP (curve d). The increase can be ascribed to the fact that AAP produced AA through the catalysis of ALP, which can capture the photogenerated holes and improve the photocurrent response. Based on the results, we can concluded that this fabricated biosensor can be used for microRNA detection.

To discuss the effect of the non-specific adsorption of the proteins to the signal, the PEC response in the absence of biotin-labelled DNA strand has been discussed (i.e., ALP/SA/ssDNA/g-C_3N_4/ITO). The results showed that the photocurrent in the absence of biotin-labelled DNA strand was significantly weaker, indicating that non-specific adsorption of the proteins does not contribute significantly to the signal.

Optimization of experimental conditions

The following parameters were optimized: (a) template DNA concentration; (b) polymerase reaction time; (c) probe concentration; (d) ALP incubation time. Respective data and Figures are given in the Electronic Supporting Material. The following experimental conditions were found to give best results: (a) template DNA concentration of 100 nM; (b) polymerase reaction time of 2.5 h; (c) probe concentration of 1 μM; (d) ALP incubation time of 70 min.

Detection performances

Under the optimal experiment conditions, the PEC response of the biosensor was analyzed with increasing microRNA-162a concentration from 0.5 to 1000 fM. As depicted in Fig. 3a, the photocurrent response increases

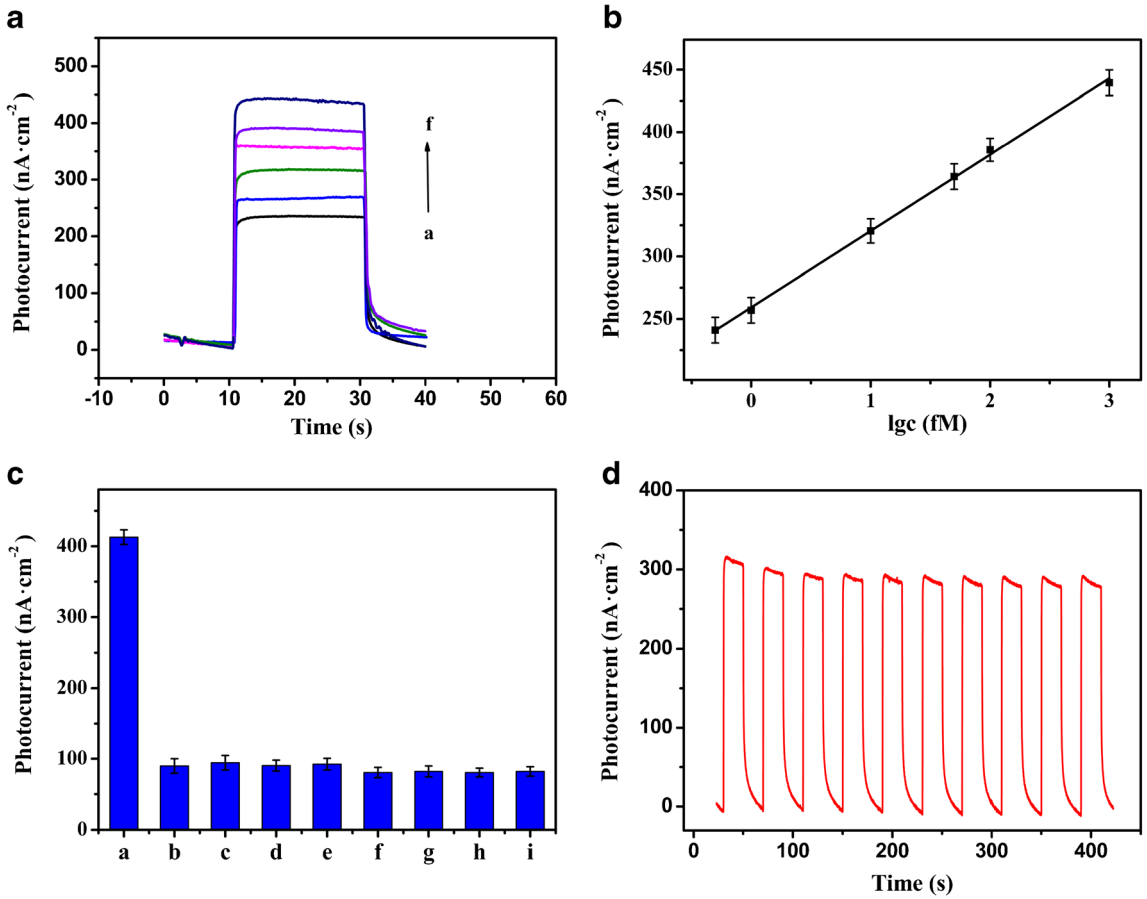

Fig. 3 **a** Photocurrent response for different concentrations of microRNA-162a. a-f, 0.5, 1, 10, 50, 100, 1000 fM. **b** Calibration curve. **c** Specificity of the biosensor. (a) microRNA-162a, (b) microRNA-166e, (c) microRNA-172a, (d) microRNA-156d, (e) microRNA-169a, (f) blank, (g) single-base mismatched microRNA, (h) three-base mismatched microRNA, (i) non-complementary DNA (The concentration of microRNA is 1 pM). **d** Time–based photocurrent responses of the biosensor in 10 mM Tris-HCl (pH 9.8) containing 50 mM KCl, 10 mM AAP and 0.1 mM $Mg(NO_3)_2$ (The concentration of microRNA is 10 fM). The photocurrent was recorded in PEC detection buffer with applied potential of −0.3 V at visible light

with the increasing microRNA-162a concentration. A linear relationship can be obtained between photocurrent and the logarithm value of microRNA-162a concentration, and the calibration curve is illustrated in Fig. 3b. The linear regression equation is I (nA·cm^{-2}) = 61.30 lg$c$ (fM) + 259.19 with the correlation coefficient of 0.9984, the photoelectrochemical sensitivity was 61.3 nA·fM^{-1}·cm^{-2} and the detection limit is 0.18 fM (S/N = 3). Compared with the linear range and the detection limit of other methods (Table 1), the fabricated biosensor shows excellent microRNA detection performance.

The selectivity of the PEC biosensor was assessed using one non-complementary DNA (1 pM), seven kinds of different microRNAs (1 pM) and blank (without any microRNA) as detection target. Seven kinds of different microRNAs include complementary microRNA (microRNA-162a), single-base mismatched microRNA, three-base mismatched microRNA, microRNA-166e, microRNA-172a, microRNA-156d and microRNA-169a. As presented in Fig. 3c, the photocurrent response for microRNA-162a is significantly higher than that of other interferents, indicating the good detection specificity of the method.

The stability is another key parameter for the biosensor, and it was also investigated (Fig. 3d). No obvious change of photocurrent response was observed with light on and off which was repeated 10 times over 400 s, and the relative standard deviation (RSD) is 2.78%, indicating a excellent stability.

Sample analysis

Chemical mutation breeding is a technique that uses chemical mutagens to induce genetic variation in plants, which can have a significant effect on the plant's character. Alkylating agent is the most important type of chemical mutagens, its mechanism is the alkylation, which is focused on nucleic acid, leading to DNA fragmentation, deletion or repair. In order to evaluate the applicability of the fabricated biosensor in real samples, the effect of EMS on the expression of microRNA-162a in the leaves of maize seedlings was investigated. To carry out this operation, maize seeds were immersed in an aqueous solution of EMS for 6 h. Total RNA was then extracted from the the leaves of maize seedlings and the photocurrent of microRNA-162a in total RNA was tested. As depicted in Fig. 4, the expression level of microRNA-162a increased after the maize seeds were incubated with 0.7% EMS. For testing the detection accuracy, the expression level of microRNA-162a was also detected by qRT-PCR. As shown in Fig. 4, the results observed by qRT-PCR are similar to the assay that we developed, indicating the reliability of our work (The corresponding data was listed in Table 2). Through this study, information about the mechanism of chemical mutation breeding is provided, in addition, information about the changes in plant traits after mutagenesis can also be provided.

Table 1 Comparison of the detection performances of the method with other methods

Methods	Linear range	LOD (fM)	Refs.
Electrochemistry	10 fM–1 nM	1.66	[24]
Electrochemistry	10 fM–10 nM	9	[25]
Electrochemistry	1 fM–100 pM	0.36	[26]
Fluorescence	1 fM–50 pM	0.27	[27]
Fluorescence	5.0 pM–50 nM	1200	[28]
Fluorescence	10 fM–0.1 nM	1.0	[29]
ECL	0.1 fM–10 pM	0.03	[30]
ECL	10 fM–100 pM	3.3	[31]
ECL	1 fM–10 pM	1	[32]
Photoelectrochemistry	350 fM–5 nM	153	[33]
Photoelectrochemistry	1 fM–500 fM	0.56	[34]
Photoelectrochemistry	10 fM–10 pM	3.5	[35]
Photoelectrochemistry	0.5 fM–1 pM	0.18	This work

Conclusions

In summary, a sensitive photoelectrochemical biosensor was developed for microRNA-162a detection based on a multiple amplification method. Based on the multiple signal amplification, the detection limit of 0.18 fM was achieved, and the photocurrent increases linearly with the concentration of microRNA-162a in the range from 0.5 fM to 1 pM. Furthermore, the application in maize seedling shown that the biosensor can exhibit good performance in actual samples. The limitation of this method was a little time-consuming for electrode fabrication. If we can decrease the fabrication time, our strategy will be a fine and

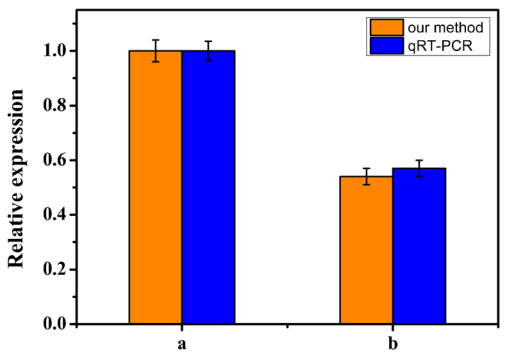

Fig. 4 The relative expression level of microRNA-162a in the leaves of maize seedlings with (a) and without (b) EMS incubation

Table 2 The expression level of microRNA-162a in the leaves of maize seedlings

Samples	Detected by this method	Detected by qRT-PCR
With EMS incubation	1	1
Without EMS incubation	0.54	0.57

rapid method for miRNA detection. Therefore, this fabricated biosensor can be applied as a prospective detection tool for microRNA-162a detection in biology research.

Acknowledgements This work was supported by the National Natural Science Foundation of China (No. 21775090), the Natural Science Foundation of Shandong Province of China (No. ZR2014BQ029), Founds of Shandong "Double Tops" Program (SYL2017XTTD15).

Compliance with ethical standards The author(s) declare that they have no competing interests.

References

1. Carthew RW, Sontheimer EJ (2009) Origins and mechanisms of miRNAs and siRNAs. Cell 136(4):642–655. https://doi.org/10.1016/j.cell.2009.01.035
2. Fiammengo R (2017) Can nanotechnology improve cancer diagnosis through miRNA detection? Biomark Med 11(1):69–86. https://doi.org/10.2217/bmm-2016-0195
3. Feng K, Liu J, Deng L, Yu H, Yang M (2018) Amperometric detection of microRNA based on DNA-controlled current of a molybdophosphate redox probe and amplification via hybridization chain reaction. Microchim Acta 185(1):28–34. https://doi.org/10.1007/s00604-017-2579-3
4. Schwarzkopf M, Pierce NA (2016) Multiplexed miRNA northern blots via hybridization chain reaction. Nucleic Acids Res 44(15):129–129. https://doi.org/10.1093/nar/gkw503
5. Choi YS, Edwards LO, Dibello A, Jose AM (2017) Removing bias against short sequences enables northern blotting to better complement RNA-seq for the study of small RNAs. Nucleic Acids Res 45(10):87–87. https://doi.org/10.1093/nar/gkx091
6. de Freitas RC, Bortolin RH, Lopes MB, Hirata MH, Hirata RD, Silbiger VN, Luchessi AD (2016) Integrated analysis of miRNA and mRNA Gene expression microarrays: influence on platelet reactivity, clopidogrel response and drug-induced toxicity. Gene 593(1):172–178. https://doi.org/10.1016/j.gene.2016.08.028
7. Pai J, Hyun S, Hyun JY, Park S-H, Kim W-J, Bae S-H, Kim N-K, Yu J, Shin I (2016) Screening of pre-miRNA-155 binding peptides for apoptosis inducing activity using peptide microarrays. J Am Chem Soc 138(3):857–867. https://doi.org/10.1021/jacs.5b09216
8. Zhou L, Wang J, Chen Z, Li J, Wang T, Zhang Z, Xie G (2017) A universal electrochemical biosensor for the highly sensitive determination of microRNAs based on isothermal target recycling amplification and a DNA signal transducer triggered reaction. Microchim Acta 184(5):1305–1313. https://doi.org/10.1007/s00604-017-2129-z
9. Liu H, Bei X, Xia Q, Fu Y, Zhang S, Liu M, Fan K, Zhang M, Yang Y (2016) Enzyme-free electrochemical detection of microRNA-21 using immobilized hairpin probes and a target-triggered hybridization chain reaction amplification strategy. Microchim Acta 183(1):297–304. https://doi.org/10.1007/s00604-015-1636-z
10. Borghei YS, Hosseini M, Ganjali MR, Hosseinkhani S (2017) Label-free fluorescent detection of microRNA-155 based on synthesis of hairpin DNA-templated copper nanoclusters by etching (top-down approach). Sensors Actuators B Chem 248:133–139. https://doi.org/10.1016/j.snb.2017.03.148
11. Wang Z, Zhang J, Chen F, Cai K (2017) Fluorescent miRNA analysis enhanced by mesopore effects of polydopamine nanoquenchers. Analyst 142(15):2796–2804. https://doi.org/10.1039/C7AN00528H
12. Li Y, Pu Q, Li J, Zhou L, Tao Y, Li Y, Yu W, Xie G (2017) An "off-on" fluorescent switch assay for microRNA using nonenzymatic ligation-rolling circle amplification. Microchim Acta 184(11):4323–4330. https://doi.org/10.1007/s00604-017-2475-x
13. Han Z, Luo M, Chen L, Pan H, Chen J, Li C (2017) A photoelectrochemical biosensor for determination of DNA based on flower rod-like zinc oxide heterostructures. Microchim Acta (8):1–9. https://doi.org/10.1007/s00604-017-2257-5
14. Kang Z, Yan X, Wang Y, Zhao Y, Bai Z, Liu Y, Zhao K, Cao S, Zhang Y (2016) Self-powered photoelectrochemical biosensing platform based on Au NPs@ZnO nanorods array. Nano Res 9(2):344–352. https://doi.org/10.1007/s12274-015-0913-9
15. Yu Z, Lv S, Ren R, Cai G, Tang D (2017) Photoelectrochemical sensing of hydrogen peroxide at zero working potential using a fluorine-doped tin oxide electrode modified with $BiVO_4$ microrods. Microchim Acta 184(3):799–806. https://doi.org/10.1007/s00604-016-2071-5
16. Wu T, Wang J, Liang W, Zang X, Wang C, Wu Q, Wang Z (2017) Single layer graphitic carbon nitride-modified graphene composite as a fiber coating for solid-phase microextraction of polycyclic aromatic hydrocarbons. Microchim Acta 184(7):2171–2180. https://doi.org/10.1007/s00604-017-2233-0
17. Yin H, Zhou Y, Li B, Li X, Yang Z, Ai S, Zhang X (2016) Photoelectrochemical immunosensor for microRNA detection based on gold nanoparticles-functionalized g-C_3N_4 and anti-DNA:RNA antibody. Sensors Actuators B Chem 222:1119–1126. https://doi.org/10.1016/j.snb.2015.08.019
18. Yu L, Wu W, Lie P, Liu Y, Zeng L (2013) Isothermal strand-displacement polymerase reaction for visual detection of the Southeast Asian-type deletion of α-thalassemia. J Mol Diagn 15(6):776–782. https://doi.org/10.1016/j.jmoldx.2013.06.003
19. Zhao B, Gong Z, Ma Z, Wang D, Jin Y (2012) Simple and sensitive microRNA labeling by terminal deoxynucleotidyl transferase. Acta Biochim Biophys Sin 44(2):129–135. https://doi.org/10.1093/abbs/gmr115
20. Wang H, Zhang Q, Yin H, Wang M, Jiang W, Ai S (2017) Photoelectrochemical immunosensor for methylated RNA detection based on g-C3N4/CdS quantum dots heterojunction and Phos-tag-biotin. Biosens Bioelectron 95:124–130. https://doi.org/10.1016/j.bios.2017.04.006
21. Wang M, Yin H, Shen N, Xu Z, Sun B, Ai S (2014) Signal-on photoelectrochemical biosensor for microRNA detection based on Bi2S3 nanorods and enzymatic amplification. Biosens Bioelectron 53:232–237. https://doi.org/10.1016/j.bios.2013.09.069
22. Li X, Zhu L, Zhou Y, Yin H, Ai S (2017) Enhanced photoelectrochemical method for sensitive detection of protein kinase A activity using TiO_2/g-C_3N_4, PAMAM dendrimer, and alkaline phosphatase. Anal Chem 89(4):2369–2376. https://doi.org/10.1021/acs.analchem.6b04184

23. Wang S, Li D, Sun C, Yang S, Guan Y, He H (2014) Synthesis and characterization of g-C_3N_4/Ag_3VO_4 composites with significantly enhanced visible-light photocatalytic activity for triphenylmethane dye degradation. Appl Catal B Environ 144:885–892. https://doi.org/10.1016/j.apcatb.2013.08.008
24. Yang J, Tang M, Diao W, Cheng W, Zhang Y, Yan Y (2016) Electrochemical strategy for ultrasensitive detection of microRNA based on MNAzyme-mediated rolling circle amplification on a gold electrode. Microchim Acta 183(11):3061–3067. https://doi.org/10.1007/s00604-016-1958-5
25. Ma W, Bo S, Lv W, Li B, Yin X, Vadgama P, Zheng L, Wang W (2016) Electrochemical determination of microRNAs based on isothermal strand-displacement polymerase reaction coupled with multienzyme functionalized magnetic micro-carriers. Biosens Bioelectron 80:344–351. https://doi.org/10.1016/j.bios.2015.12.064
26. Li B, Liu F, Peng Y, Zhou Y, Fan W, Yin H, Ai S, Zhang X (2016) Two-stage cyclic enzymatic amplification method for ultrasensitive electrochemical assay of microRNA-21 in the blood serum of gastric cancer patients. Biosens Bioelectron 79:307–312. https://doi.org/10.1016/j.bios.2015.12.051
27. Yin HS, Li BC, Zhou YL, Wang HY, Wang MH, Ai SY (2017) Signal-on fluorescence biosensor for microRNA-21 detection based on DNA strand displacement reaction and Mg^{2+}-dependent DNAzyme cleavage. Biosens Bioelectron 96:106–112. https://doi.org/10.1016/j.bios.2017.04.049
28. Borghei Y-S, Hosseini M, Ganjali MR (2017) Fluorometric determination of microRNA via FRET between silver nanoclusters and CdTe quantum dots. Microchim Acta 184(12):4713–4721. https://doi.org/10.1007/s00604-017-2512-9
29. Zhou Y, Li B, Wang M, Wang J, Yin H, Ai S (2017) Fluorometric determination of microRNA based on strand displacement amplification and rolling circle amplification. Microchim Acta 184(11):4359–4365. https://doi.org/10.1007/s00604-017-2450-6
30. Yu YQ, Wang JP, Zhao M, Hong LR, Chai YQ, Yuan R, Zhuo Y (2016) Target-catalyzed hairpin assembly and intramolecular/intermolecular CO-reaction for signal amplified electrochemiluminescent detection of microRNA. Biosens Bioelectron 77:442–450. https://doi.org/10.1016/j.bios.2015.09.056
31. Xu Z, Liao L, Chai Y, Wang H, Yuan R (2017) Ultrasensitive electrochemiluminescence biosensor for microRNA detection by 3D DNA. walking machine based target conversion and distance-controllable signal quenching and enhancing. Anal Chem 89(16):8282–8287. https://doi.org/10.1021/acs.analchem.7b01409
32. Liu T, Chen X, Hong C-Y, Xu X-P, Yang H-H (2014) Label-free and ultrasensitive electrochemiluminescence detection of microRNA based on long-range self-assembled DNA nanostructures. Microchim Acta 181(7):731–736. https://doi.org/10.1007/s00604-013-1113-5
33. Tu W, Cao H, Long Z, Bao J, Liu X, Dai Z (2016) Dual signal amplification using gold nanoparticles-enhanced zinc selenide nanoflakes and P19 protein for ultrasensitive photoelectrochemical biosensing of microRNA in cell. Anal Chem 88(21):10459–10465. https://doi.org/10.1021/acs.analchem.6b02381
34. Li B, Li X, Wang M, Yang Z, Yin H, Ai S (2015) Photoelectrochemical biosensor for highly sensitive detection of microRNA based on duplex-specific nuclease-triggered signal amplification. J Solid State Electrochem 19(5):1301–1309. https://doi.org/10.1007/s10008-015-2747-5
35. Wang M, Yang Z, Guo Y, Wang X, Yin H, Ai S (2015) Visible-light induced photoelectrochemical biosensor for the detection of microRNA based on Bi2S3 nanorods and streptavidin on an ITO electrode. Microchim Acta 182(1):241–248. https://doi.org/10.1007/s00604-014-1324-4